

Helical Edge Modes near Transition to Topological Insulator with Indirect Gap

Shijun Mao^{1,2} and Yoshio Kuramoto¹

Department of Physics, Tohoku University, Sendai 980-8578, Japan¹
Department of Physics, Tsinghua University, Beijing 100084, P.R.China²

(Dated: November 9, 2010)

Helical edge modes are characteristic of topological insulators in two dimensions. This paper demonstrates that helical edge modes remain across transitions to ordinary insulators or to semimetals under certain condition. Straight and zigzag edges are considered in a tight-binding model on square lattice. We focus on the case of indirect gap in bulk topological insulators, and obtain the spectrum of edge modes on both sides of transitions. For straight edge, the helical edge mode in topological insulators with strong particle-hole asymmetry has a reentrant region in momentum space. Edge modes show up even in ordinary insulators, but are absent in semimetals. In zigzag edge, the helical edge mode survives in both semimetals and ordinary insulators. However, the edge modes are absent inside the energy gap of ordinary insulators. All results are obtained analytically.

PACS numbers: 73.20.-r, 73.20.At, 73.63.Hs

Keywords: topological insulator, edge mode, indirect gap, particle-hole symmetry, semimetal, annihilator

I. INTRODUCTION

In recent intensive study of topological insulators (TI), property of helical edge (2D TI) or surface (3D TI) states is one of the key topics. It has been shown that these states are robust against interaction and disorder [1, 2]. The dissipationless spin current has potential application in spintronics. In experiments for topological insulator materials, some materials are actually *bulk metals*, but still support topological surface states, such as Sb[3, 4], Bi_{0.91}Sb_{0.09}[5, 6], Bi_{2-x}Mn_xTe₃[7] and Bi₂Se₃ [8, 9]. This kind of surface modes in (semi)metallic systems deserves further study, especially as to their implication to the topologically nontrivial and trivial systems. With realistic energy bands for Bi₂Se₃, which are obtained by *ab initio* band calculation, the spectrum of helical surface modes has already been derived numerically [10]. However, except for the low-energy part, further property of the surface mode, such as the existence region in momentum space, has not been discussed. Note that the topological argument about the robustness of the mode applies only to the energy region where bulk excitations are absent. In this paper we are interested in global property of the helical modes including the region overlapping with bulk excitations.

One of the widely used models for 2D TI has been proposed by Bernevig, Hughes and Zhang[11], and is called the BHZ model. Helical edge states have been further studied using the resultant continuum model [12, 13] and the lattice regularized model [14–16]. In these previous papers, the particle-hole symmetry has been assumed. Namely, the conduction and valence bands have the same spectrum except for the sign. Hence the direct energy gap follows. In materials such as Sb and Bi_{0.91}Sb_{0.09}, however, the energy gap or overlap involves different positions in momentum space. Hence theoretical study beyond the particle-hole symmetric case is of practical interest.

In this paper, we study these helical states in both

topologically nontrivial and trivial cases. In order to clarify the characteristics associated with the particle-hole asymmetry in the simplest manner, we take the BHZ model on the square lattice, and derive the spectrum of helical modes analytically. We consider a strip geometry of the 2D system with straight and zigzag edges as in ref.[16], and generalize its method for deriving helical edge states to particle-hole asymmetric case.

The paper is organized as follows: In §2, we review the particle-hole asymmetric BHZ tight-binding model, paying attention to both direct and indirect gap-closing in 2D Brillouin zone (BZ). Sections 3 and 4 are devoted to the straight edge and zigzag edge systems, respectively. We analytically derive spectrum of helical edge states in particle-hole asymmetric system. In straight edge case, edge mode is present in TI and, under appropriate conditions, also in ordinary insulators (OI). However, it's absent in semimetals (SM). In zigzag edge case, helical edge states survive in each case of TI, OI, and SM. The summary and outlook are given in §5.

II. PARTICLE-HOLE ASYMMETRIC BHZ MODEL

We consider the BHZ model given by the following block diagonalized 4×4 matrix:

$$H(\vec{k}) = \begin{bmatrix} h(\vec{k}) & 0 \\ 0 & h^*(-\vec{k}) \end{bmatrix}, \quad (1)$$

where $\vec{k} = (k_x, k_y)$ is a 2D crystal momentum. The lower-right block $h^*(-\vec{k})$ for down-spin is deduced from the upper-left block $h(\vec{k})$ for up-spin by time-reversal transformation. We parametrize $h(\vec{k})$ as

$$h(\vec{k}) = \epsilon(\vec{k})\sigma_0 + \vec{d}(\vec{k}) \cdot \vec{\sigma} = \begin{bmatrix} \epsilon + d_z & d_x - id_y \\ d_x + id_y & \epsilon - d_z \end{bmatrix}, \quad (2)$$

where σ_0 is the 2×2 unit matrix in the pseudo-spin space representing the two kinds of orbitals, and $\vec{\sigma}$ is

the vector composed of the Pauli matrices σ_x, σ_y and σ_z . We write $\sigma_0 = 1$ hereafter unless confusion arises. We consider the BHZ model over the whole BZ of the square lattice. Then the energy parameters are given by the tight-binding form as

$$\epsilon(\vec{k}) = C - 2D(2 - \cos k_x - \cos k_y) \quad (3)$$

$$d_x(\vec{k}) = A \sin k_x, \quad d_y(\vec{k}) = A \sin k_y, \quad (4)$$

$$d_z(\vec{k}) = \Delta - 2B(2 - \cos k_x - \cos k_y), \quad (5)$$

with the lattice constant a set to unity[11].

The bulk energy $E_b(\vec{k})$ is obtained as

$$E_{b\pm}(\vec{k}) = \epsilon(\vec{k}) \pm \left\{ A^2 (\sin^2 k_x + \sin^2 k_y) + [\Delta - 4B + 2B(\cos k_x + \cos k_y)]^2 \right\}^{1/2}, \quad (6)$$

It is clear that finite $\epsilon(\vec{k})$ breaks the particle-hole symmetry. Since C in Eq.(3) merely describes the energy shift of the origin, we put $C = 0$ for simplicity. As in our previous paper[16], we use B as the unit of energy and put $B = 1$ hereafter.

The change of Δ will cause transition between TI and OI. With inversion symmetry, the direct gap can close only at time-reversal invariant points, namely at $\Gamma = (0, 0)$, $X = (\pi, 0)$, $X' = (0, \pi)$ and $M = (\pi, \pi)$ [17], where bulk energies become

$$E_{b\pm}(0, 0) = \pm|\Delta|, \quad (7)$$

$$E_{b\pm}(0, \pi) = -4D \pm |\Delta - 4| = E_{b\pm}(\pi, 0), \quad (8)$$

$$E_{b\pm}(\pi, \pi) = -8D \pm |\Delta - 8|. \quad (9)$$

As one varies the parameter Δ , the direct gap closes at Γ , for example, when $\Delta = 0$. Similarly the gap closes at X (also X') with $\Delta = 4$, and at M with $\Delta = 8$.

Due to finite $\epsilon(\vec{k})$, it is also possible to have the indirect gap-closing. For example, we obtain $E_{b+}(0, \pi) = -\Delta$ with $0 < \Delta < 4$ and $D = 1$ from Eq.(8), which becomes the same as $E_{b-}(0, 0) = -\Delta$. Then the transition occurs between TI and SM at $D = 1$ for $0 < \Delta < 4$.

In this paper we only deal with edge mode with up-spin and confine to the case $A, D > 0$ and $\Delta < 4$, since the down-spin part is obtained by using the time-reversal symmetry. Note that the result for negative D is obtained by changing the role of conduction and valence bands. On the other hand, the case $\Delta > 4$ is understood by changing the role of Γ and M points in the Brillouin zone[16].

III. STRAIGHT EDGE

A. Analytic solution of spectrum and wave function

Let us first consider a straight edge geometry (see Fig. 1a), in which electrons are confined to N_r rows in a

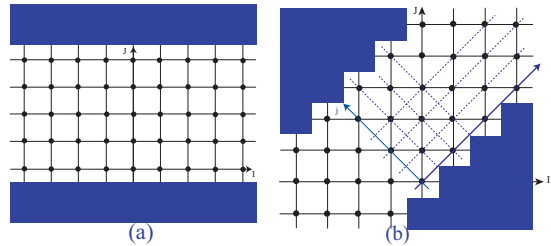


FIG. 1. (Color online) (a) Straight edge system with boundaries in (1,0) direction. (b) Zigzag edge system with boundaries in (1,1) direction.

strip between $y = 1$ and $y = N_r$, i.e., the two edges are along x -axis. Translational invariance along x -axis allows for constructing a 1D tight-binding Hamiltonian $h_{01}(k)$ with $k = k_x$ in terms of the creation $c_J^\dagger(k)$ and annihilation $c_J(k)$ operators with row index J , which are two-component vectors in the pseudo-spin space. For up spin, the 1D model h_\uparrow is obtained as

$$h_\uparrow = \sum_k h_{01}(k), \quad (10)$$

$$h_{01}(k) = \sum_J c_J^\dagger(k) \hat{\mathcal{E}}(k) c_J(k) + \sum_J \left[c_J^\dagger(k) \hat{t}_y c_{J+1}(k) + h.c. \right] \quad (11)$$

where $\hat{\mathcal{E}}(k)$ and \hat{t}_y are given by

$$\hat{\mathcal{E}}(k) = (-4D + 2D \cos k) + A \sin k \sigma_x + (\Delta_B + 2 \cos k) \sigma_z, \quad (12)$$

$$\hat{t}_y = -i \frac{A}{2} \sigma_y + \sigma_z + D. \quad (13)$$

Here and in the following, we use the notation $\Delta_B \equiv \Delta - 4$. The corresponding Schrödinger equation is given by

$$\hat{\mathcal{E}}(k) \Psi_J + \hat{t}_y \Psi_{J-1} + \hat{t}_y^\dagger \Psi_{J+1} = E(k) \Psi_J \quad (14)$$

where Ψ_J is the two-component amplitude with row index J . The straight edges along the $J = 1$ row and $J = N_r$ row can be implemented by open boundary condition $\Psi_0 = \Psi_{N_r+1} = 0$.

We consider the thermodynamic limit $N_r \rightarrow \infty$, and try an edge state solution with property: $\Psi_{J+1} = \lambda \Psi_J = \lambda^{J+1} \Psi$ with $|\lambda| < 1$ [18, 19]. Here λ is a complex number in general. Then Eq.(14) can be written in the following form:

$$\left[\hat{\mathcal{E}}(k) + \lambda \hat{t}_y^\dagger + \lambda^{-1} \hat{t}_y \right] \Psi \equiv P_{01}(\lambda, k) \Psi = E(k) \Psi. \quad (15)$$

Although $P_{01}(\lambda, k)$ is a 2×2 matrix, there is at most one solution Ψ for the helical edge mode in Eq.(15). We decompose $P_{01}(\lambda, k)$ into the Hermitian part and the rest

called the annihilator[16]. The absence of the particle-hole symmetry in the present case requires a little more complicated procedure than before [16]. Let us first introduce a parameter ϕ and make the following transformation:

$$\sigma_X = \cos \phi \sigma_x + \sin \phi \sigma_z \quad (16)$$

$$\sigma_Z = -\sin \phi \sigma_x + \cos \phi \sigma_z \quad (17)$$

Then, we have

$$\hat{\mathcal{E}}(k) = \mathcal{E}_0 + \mathcal{E}_1 \sigma_X + \mathcal{E}_3 \sigma_Z, \quad (18)$$

$$\mathcal{E}_0 = -4D + 2D \cos k, \quad (19)$$

$$\mathcal{E}_1 = A \sin k \cos \phi + (\Delta_B + 2 \cos k) \sin \phi, \quad (20)$$

$$\mathcal{E}_3 = -A \sin k \sin \phi + (\Delta_B + 2 \cos k) \cos \phi, \quad (21)$$

$$\begin{aligned} \lambda \hat{t}_y^\dagger + \lambda^{-1} \hat{t}_y &= \frac{i}{2} A (\lambda - \lambda^{-1}) \sigma_y + \cos \phi (\lambda + \lambda^{-1}) \sigma_Z \\ &+ (\lambda + \lambda^{-1}) (\sin \phi \sigma_X + D). \end{aligned} \quad (22)$$

Now we decompose $P_{01}(\lambda, k)$ in Eq.(15) as

$$P_{01} = H_{01} + F_{01}, \quad (23)$$

where the Hermitian part H_{01} is chosen as combination of σ_0 ($= 1$) and σ_X terms. The eigenstate Ψ of H_{01} obeys the relation $\sigma_X \Psi = s \Psi$ with $s = \pm 1$. Furthermore, σ_y and σ_Z terms combine to form the annihilator F_{01} [16]. Namely we obtain

$$H_{01} \Psi = E(k) \Psi, \quad F_{01} \Psi = 0, \quad (24)$$

$$H_{01} = \mathcal{E}_0 + \mathcal{E}_1 \sigma_X + (\lambda + \lambda^{-1}) (\sin \phi \sigma_X + D), \quad (25)$$

$$F_{01} = i \frac{A}{2} (\lambda - \lambda^{-1}) \sigma_y + [\mathcal{E}_3 + \cos \phi (\lambda + \lambda^{-1})] \sigma_Z, \quad (26)$$

In view of $E(k)$ being real, and the parameter λ being complex in general, we require in H_{01} the condition

$$(\sin \phi \sigma_X + D) \Psi = 0, \quad (27)$$

which determines ϕ as

$$\sin \phi = -sD. \quad (28)$$

Then $E(k)$ of the edge mode reads

$$E(k) = s\mathcal{E}_1 + \mathcal{E}_0. \quad (29)$$

The condition for F_{01} , which is given by Eq.(26), to form the annihilator $\sigma_y + is\sigma_Z$ reads

$$\mathcal{E}_3 + \cos \phi (\lambda + \lambda^{-1}) = -s \frac{A}{2} (\lambda - \lambda^{-1}), \quad (30)$$

which determines λ since ϕ has already been fixed by Eq.(28). The solutions $\lambda = \lambda_{s\pm}(k)$ are given by

$$\lambda_{s\pm}(k) = \frac{-\mathcal{E}_3 \pm \sqrt{\mathcal{E}_3^2 - 4 \cos^2 \phi + A^2}}{2 \cos \phi + sA}, \quad (31)$$

with $\cos \phi = \sqrt{1 - D^2}$. The dependence on k comes only through \mathcal{E}_3 . For complex λ , we obtain

$$|\lambda_{s\pm}|^2 = \frac{2\sqrt{1 - D^2} - sA}{2\sqrt{1 - D^2} + sA}, \quad (32)$$

which does not depend on k , and should be less than unity. Therefore, we must choose $s = 1$ that corresponds to the right-going mode. We obtain the spectrum:

$$E_\uparrow(k) = \mathcal{E}_1 + \mathcal{E}_0 = -D\Delta + A\sqrt{1 - D^2} \sin k. \quad (33)$$

In the case of $D = 0$, the spectrum is reduced to $A \sin k$, which was already obtained [14–16]. The constant term $-D\Delta$ can be canceled by the chemical potential. Then the zero mode occurs at $k = 0$. Otherwise the zero mode has a finite momentum. The two-component wave function is given by

$$\Psi_J = (\lambda_+^J - \lambda_-^J) \begin{pmatrix} \sqrt{1 - D} \\ \sqrt{1 + D} \end{pmatrix}, \quad (34)$$

apart from the normalization factor. Hereafter we use notation $\lambda_\pm = \lambda_{1\pm}$, since only the case of $s = 1$ is relevant.

Fig.2 (a) shows the spectrum of the system including both h_\uparrow and h_\downarrow , *i.e.*, two helical modes. The bulk spectrum is obtained by projecting the 2D spectrum for a finite but large system into 1D BZ of the straight edge. The parameter $|\lambda_\pm|$ is shown in Fig.2 (b). The edge modes are present only if $|\lambda| < 1$ is satisfied for both λ_\pm . It is clear from Fig.2(b) that the momentum range for the edge mode is split into two; one is localized around center of BZ, and the other allows for a reentrant edge mode [15, 16]. Furthermore, the two parts have exactly the same width for the momentum range. This fact can be understood by writing \mathcal{E}_3 in Eq.(21) as

$$\begin{aligned} \mathcal{E}_3 - \Delta_B \sqrt{1 - D^2} &= AD \sin k + 2\sqrt{1 - D^2} \cos k \\ &= \sqrt{A^2 D^2 + 4(1 - D^2)} \sin(k + \alpha), \end{aligned} \quad (35)$$

with $\tan \alpha = 2\sqrt{1 - D^2}/(AD)$. This expression shows that \mathcal{E}_3 is symmetric about

$$k = k_c = \pi/2 - \alpha = \arctan \frac{AD}{2\sqrt{1 - D^2}}, \quad (36)$$

which becomes 1.18 with the chosen values of $A = 1$ and $D = 0.98$. Hence, according to Eq.(31), the value of λ_\pm is also symmetric around k_c as seen from Fig.2(b). The allowed momentum range for the edge mode with $|\lambda_\pm| < 1$ is also symmetric around k_c .

B. Transition to semimetals

Fig.3 shows the critical case with $D = 1$ where the minimum value of conduction band is equal to the maximum

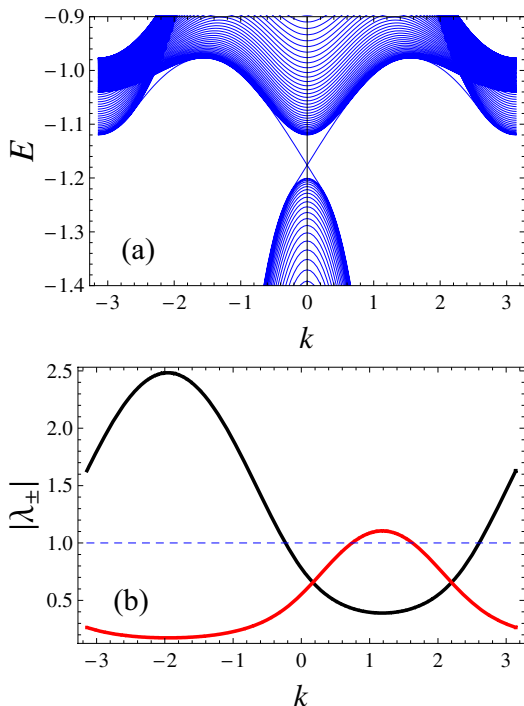


FIG. 2. (Color online) (a) Energy band $E(k)$ and (b) parameters $|\lambda_-|$ (red) and $|\lambda_+|$ (black) in straight edge system with $\Delta = 1.2$, $A = 1$, $D = 0.98$. Here, parameter $|\lambda_{\pm}|$ corresponds to right-going branch of edge mode.

value of valence band:

$$E_{b+}|_{min} = E_{b+}(0, \pi) = E_{b+}(\pi, \pi) = -\Delta \quad (37)$$

$$E_{b-}|_{max} = E_{b-}(0, 0) = -\Delta. \quad (38)$$

For the parameter λ_{\pm} , we obtain

$$\lambda_{\pm} = -\sin k \pm \sqrt{1 + \sin^2 k}, \quad (39)$$

which means $\lambda_- \leq -1$ for $0 \leq k \leq \pi$, and $\lambda_+ \geq 1$ for $-\pi \leq k \leq 0$. Therefore, the edge mode is absent for any momentum in the critical case.

For $D > 1$, the bulk system becomes a semimetal. Fig.4 shows the spectrum in this case with $D = 1.1$. Because we have $\sin \phi = -D < -1$, the edge mode is absent.

Let us summarize the situation with changing D for the straight edge: With $D = 0$, the system is topologically nontrivial insulator with particle-hole symmetry. For $D > 0$, the particle-hole symmetry is broken and the shape of valence and conduction bands become different. As getting close to the critical case with $D = 1$, the spectrum of the edge mode separates into two parts with the same width in the 1D momentum space, and both parts shrink simultaneously with further increase of D . At $D = 1$, associated with closing of the bulk band gap, edge modes disappear in the whole BZ. With $D > 1$, the system enters into semimetals where no edge modes are present for the straight edge.

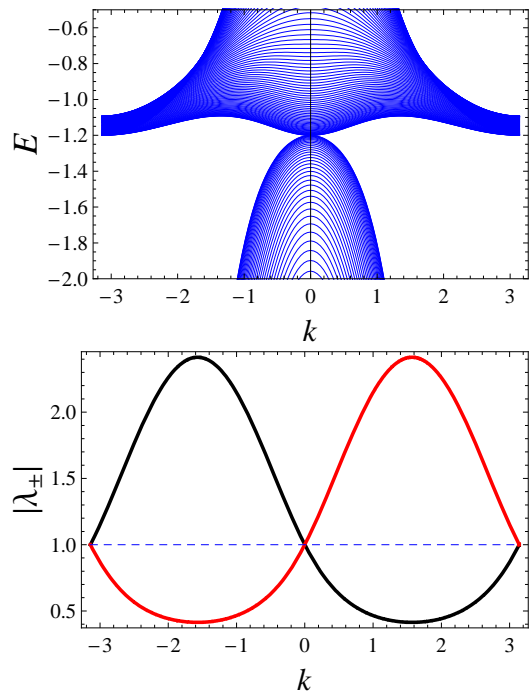


FIG. 3. (Color online) Energy band $E(k)$ and parameter $|\lambda_{\pm}|$ in straight edge system with $\Delta = 1.2$, $A = 1$, $D = 1.0$. Here, parameter $|\lambda_{\pm}|$ corresponds to right-going branch of edge mode.

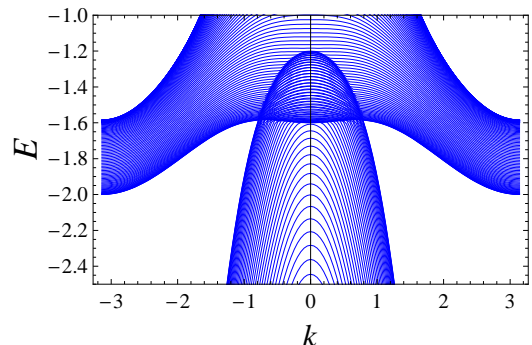


FIG. 4. (Color online) Energy band $E(k)$ of straight edge system with $\Delta = 1.2$, $A = 1$, $D = 1.1$.

C. Edge mode in ordinary insulators

We consider the edge mode in ordinary (topologically trivial) insulators (OI). In the particle-hole symmetric system, there is no edge modes [11, 14]. In the present case, edge modes can show up even in OI depending on the value of D . The presence of edge modes in OI can be analyzed conveniently by considering two limiting cases: (i) particle-hole symmetric case with $D = 0$, where we obtain $\mathcal{E}_3 = \Delta_B + 2 \cos k$; (ii) critical case with $D = 1$, where the bulk energy gap closes and edge mode disap-

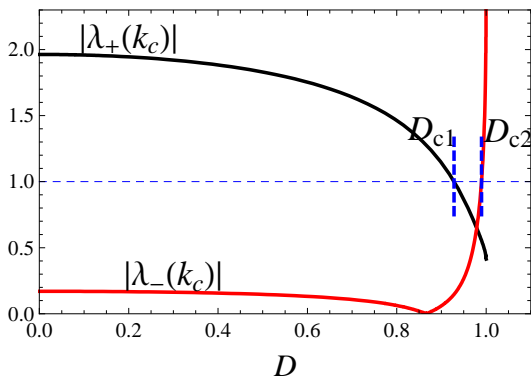


FIG. 5. (Color online) $|\lambda_{\pm}(k_c)|$ as a function of D , with $\Delta = -1.2$ and $A = 1$. Helical edge modes appear for $D_{c1} < D < 1$ although system is an ordinary insulator. Especially, for $D_{c2} < D < 1$, helical edge mode contains two separate parts. We obtain $D_{c1} = 0.93$ and $D_{c2} = 0.99$ with present choice of parameters.

pears. Here we obtain $\mathcal{E}_3 = A \sin k$. In order to derive the momentum region allowing for edge modes, we consider extrema of λ_{\pm} at $k = k_c$. We obtain from Eq.(35)

$$\mathcal{E}_3 = \Delta_B \sqrt{1 - D^2} + \sqrt{A^2 D^2 + 4(1 - D^2)}, \quad (40)$$

which is negative for

$$\Delta_B < - \left(\frac{A^2 D^2}{1 - D^2} + 4 \right)^{1/2}. \quad (41)$$

In the case of $\mathcal{E}_3 < 0$ we obtain $|\lambda_+(k_c)| > |\lambda_-(k_c)|$, and otherwise opposite inequality.

Fig.5 plots the parameters $|\lambda_{\pm}(k_c)|$ given by Eq.(31) as a function of D . We set $\Delta = -1.2$, or $\Delta_B = -5.2$, which makes the system OI. Helical edge modes appear for $D_{c1} < D < 1$ where the boundary D_{c1} are given by solution of the condition

$$\lambda_+(k_c) = 1. \quad (42)$$

With D increasing from zero to unity, $|\lambda_+(k_c)|$ decreases, as seen in Fig 5. As long as $D < D_{c1}$, we have the relation $|\lambda_+(k_c)| > 1$, and no edge modes.

At $D = D_{c1}$, we obtain $|\lambda_-(k_c)| < |\lambda_+(k_c)| = 1$, and the edge mode begins to show up. Fig.6 shows an example of the spectrum in the OI with $\Delta = -1.2$ and $A = 1$. Here edge modes appear in the middle of the BZ without the reentrant behavior.

With further increase of D , we come close to the limiting case (ii), and have the reversed relation $|\lambda_+(k_c)| < |\lambda_-(k_c)|$. At $D = D_{c2}$, we obtain $|\lambda_-(k_c)| = 1$. Then the edge mode vanishes at $k = k_c$, but is still present on both sides of k_c . Thus, with $D_{c2} < D < 1$, edge mode contains two separate parts. Fig.7 shows the spectrum and $|\lambda_{\pm}|$ corresponding to this case. The separate momentum regions, which are symmetric around k_c , shrink

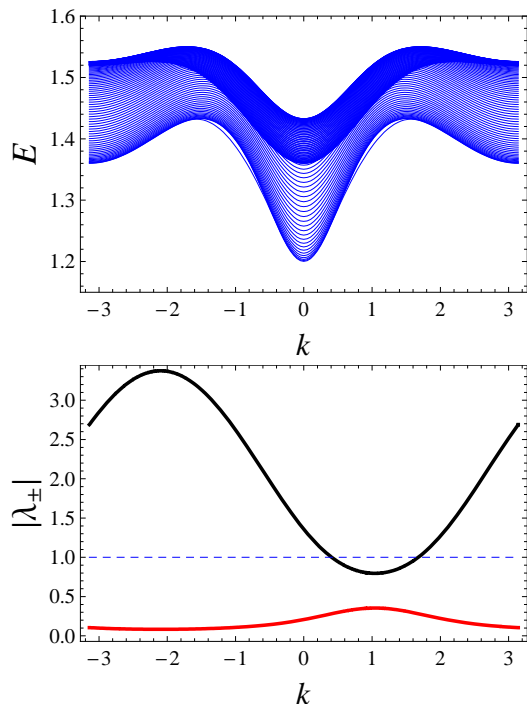


FIG. 6. (Color online) Conduction band $E(k)$ and parameter $|\lambda_{\pm}|$ for $D = 0.96$, $\Delta = -1.2$, $A = 1$. The parameter $|\lambda_{\pm}|$ corresponds to right-going branch of edge mode, which does not have the reentrant behavior.

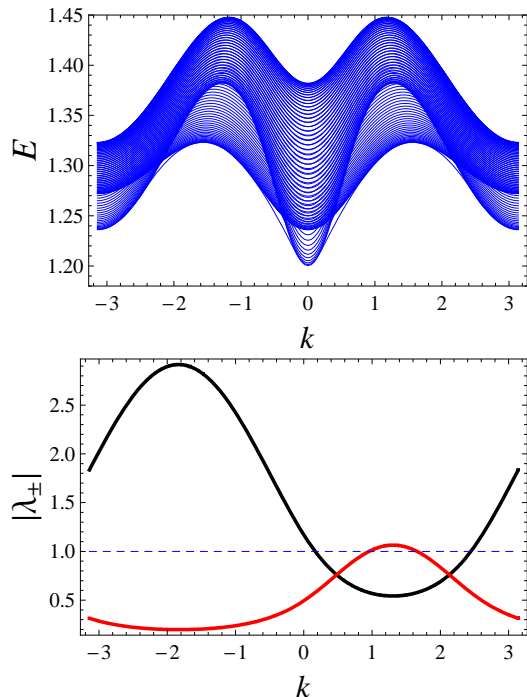


FIG. 7. (Color online) Conduction band $E(k)$ and parameter $|\lambda_{\pm}|$ for $D = 0.991$. Other parameters are the same as those in Fig.6. Reentrant modes are present in this case.

simultaneously until $D = 1$ is reached, where edge modes disappear completely. In Fig.7 we obtain $k_c = 1.307$ from Eq.(36).

IV. ZIGZAG EDGE

A. Analytic solution

Let us now consider the zigzag edge geometry, as illustrated in Fig.1(b). Electrons are confined in a diagonal strip: $1 \leq y - x \leq N_r$, provided the edges are placed at $y - x = 1$ and $y - x = N_r$, normal to the $(1, -1)$ -direction. Translational invariance remains along the $(1, 1)$ -direction. Bulk energy E_b in terms of variables $\kappa = (k_x + k_y)/2$ and $\xi = (k_x - k_y)/2$ is obtained from Eq.(6) as

$$E_{b\pm}(\kappa, \xi) = -4D + 4D \cos \kappa \cos \xi \pm [2A^2 (\sin^2 \kappa \cos^2 \xi + \cos^2 \kappa \sin^2 \xi) + (\Delta_B + 4 \cos \kappa \cos \xi)^2]^{1/2}. \quad (43)$$

The Schrödinger equation for the edge mode analogous to Eq.(14) reads:

$$\hat{\mathcal{E}}_{11} \Phi_j + \hat{t}_{11} \Phi_{j-1} + \hat{t}_{11}^\dagger \Phi_{j+1} = E_\uparrow(\kappa) \Phi_j, \quad (44)$$

where

$$\begin{aligned} \hat{\mathcal{E}}_{11} &= -4D + \Delta_B \sigma_z, \\ \hat{t}_{11} &= \frac{A}{\sqrt{2}} \sin \kappa \sigma_X - i \frac{A}{\sqrt{2}} \cos \kappa \sigma_Y, \\ &+ 2 \cos \kappa \sigma_z + 2D \cos \kappa, \end{aligned} \quad (45)$$

and we have introduced

$$\sigma_X = \frac{1}{\sqrt{2}} (\sigma_x + \sigma_y) \quad \sigma_Y = \frac{1}{\sqrt{2}} (\sigma_y - \sigma_x). \quad (47)$$

Here the conserved momentum is $\kappa = (k_x + k_y)/2$, with $-\pi/2 < \kappa < \pi/2$. We impose the boundary condition: $\Phi_0 = \Phi_{N_r+1} = 0$ for zigzag edge geometry, and consider the thermodynamic limit $N_r \rightarrow \infty$.

Assuming eigenstate of Eq.(44) with property $\Phi_j = \lambda \Phi_{j-1} = \lambda^j \Phi$, where $|\lambda| < 1$, we obtain

$$\left[\hat{\mathcal{E}}_{11} + \lambda \hat{t}_{11}^\dagger(\kappa) + \lambda^{-1} \hat{t}_{11}(\kappa) \right] \Phi = P_{11}(\lambda, \kappa) \Phi = E_\uparrow(\kappa) \Phi \quad (48)$$

In order to construct the annihilator F_{11} for the zigzag edge, we introduce further transformation:

$$\sigma_{\theta x} = \cos \theta \sigma_X + \sin \theta \sigma_z, \quad (49)$$

$$\sigma_{\theta z} = -\sin \theta \sigma_X + \cos \theta \sigma_z. \quad (50)$$

Then, we have

$$\begin{aligned} \hat{\mathcal{E}}_{11} &= -4D + \Delta_B (\sigma_{\theta x} \sin \theta + \sigma_{\theta z} \cos \theta), \\ \hat{t}_{11} &= \left(\frac{A}{\sqrt{2}} \sin \kappa \cos \theta + 2 \cos \kappa \sin \theta \right) \sigma_{\theta x} - i \frac{A}{\sqrt{2}} \sigma_y \cos \kappa \\ &+ \left(-\frac{A}{\sqrt{2}} \sin \kappa \sin \theta + 2 \cos \kappa \cos \theta \right) \sigma_{\theta z} + 2D \cos \kappa. \end{aligned} \quad (51)$$

We decompose P_{11} in Eq.(48) as $P_{11} = H_{11} + F_{11}$ where

$$H_{11} = (\Delta_B \sin \theta \sigma_{\theta x} - 4D) + (\lambda + \lambda^{-1}) (\gamma_1 \sigma_{\theta x} + 2D \cos \kappa), \quad (52)$$

$$F_{11} = \gamma_2 \sigma_y + \gamma_3 \sigma_{\theta z}, \quad (54)$$

with

$$\gamma_1 = \frac{A}{\sqrt{2}} \sin \kappa \cos \theta + 2 \cos \kappa \sin \theta, \quad (55)$$

$$\gamma_2 = -i \frac{A}{\sqrt{2}} \cos \kappa (\lambda^{-1} - \lambda), \quad (56)$$

$$\gamma_3 = \Delta_B \cos \theta + (\lambda + \lambda^{-1}) \left(-\frac{A}{\sqrt{2}} \sin \kappa \sin \theta + 2 \cos \kappa \cos \theta \right). \quad (57)$$

Note that H_{11} contains non-Hermitian part due to the complex parameter λ . Since H_{11} should have real eigenenergy $E_\uparrow(\kappa)$, we require the complex part in H_{11} to be ineffective:

$$(\gamma_1 \sigma_{\theta x} + 2D \cos \kappa) \Phi = 0, \quad (58)$$

with $\sigma_{\theta x} \Phi = s \Phi$. Then the parameter θ is determined as

$$\sin \theta = \frac{-8sD - \text{sgn} \kappa \sqrt{A^4 \tan^4 \kappa + 8A^2 (1 - D^2) \tan^2 \kappa}}{8 + A^2 \tan^2 \kappa}. \quad (59)$$

$$\cos \theta = \sqrt{1 - \sin^2 \theta} (> 0). \quad (60)$$

The eigenenergy is given by

$$E_\uparrow(\kappa) = s \Delta_B \sin \theta - 4D, \quad (61)$$

where $s = +1$ should be chosen for the edge mode, as shown below. From Eq.(59) we obtain the limiting behavior:

$$\sin \theta \rightarrow \begin{cases} -\text{sgn} \kappa & (\kappa \rightarrow \pm\pi/2) \\ -sD, & (\kappa \rightarrow 0) \end{cases} \quad (62)$$

which gives $E_\uparrow(0) = -D\Delta$ and $E_\uparrow(\pi/2) = -\Delta + 4(1 - D)$.

The corresponding annihilator F_{11} in Eq.(54) should be proportional to $\sigma_y + is\sigma_{\theta z}$, which requires

$$\Delta_B \cos \theta + (\lambda + \lambda^{-1}) R = s \frac{A}{\sqrt{2}} \cos \kappa (\lambda^{-1} - \lambda). \quad (63)$$

with

$$R = -\frac{A}{\sqrt{2}} \sin \kappa \sin \theta + 2 \cos \kappa \cos \theta. \quad (64)$$

The solution is given by

$$\lambda_{s\pm}(\kappa) = \frac{-\Delta_B \cos \theta \pm \sqrt{\Delta_B^2 \cos^2 \theta + 2A^2 \cos^2 \kappa - 4R^2}}{2R + s\sqrt{2}A \cos \kappa}, \quad (65)$$

which leads, for complex λ , to

$$|\lambda_{s\pm}(\kappa)|^2 = \frac{2R - s\sqrt{2}A \cos \kappa}{2R + s\sqrt{2}A \cos \kappa}. \quad (66)$$

In order to choose the appropriate branch out of $s = \pm 1$, we put $\kappa = 0$ and obtain $R = 2 \cos \theta > 0$. In this case the quantity

$$|\lambda_{s\pm}|^2 = (4 \cos \theta - s\sqrt{2}A)/(4 \cos \theta + s\sqrt{2}A)$$

is less than unity only with $s = +1$.

We now consider the case $\kappa = \pm\pi/2$. From Eq.(64) we obtain $R = A/\sqrt{2}$, and then

$$\lambda_{s\pm}(\pm\pi/2) = \pm i. \quad (67)$$

Since $\lambda_{s\pm}(\pm\pi/2)$ is complex, we obtain $|\lambda_{1\pm}| < 1$ near the zone boundary. This property means that edge mode near zone boundary is stable against transition from TI to SM (or OI). However, its existent region shrinks with increasing D . Hereafter, we use notation $\lambda_{\pm} = \lambda_{1\pm}(\kappa)$.

B. Edge modes in TI and topologically trivial cases

In this subsection we fix $\Delta = \pm 1.2$, $A = 1$, which realizes TI with $0 < D < 1$ and $\Delta > 0$. Note that $\kappa = 0$ is always a crossing point of two helical modes, as a result of time-reversal symmetry of the system. Hence this property is robust against particle-hole symmetry breaking as long as the system is still in TI. However, the existent regions of edge mode will shrink with increasing D .

Fig.8 shows the spectrum and $|\lambda_{\pm}|$ in the case of $D = 0.9$, $\Delta = 1.2$. As shown in the lower panel, we always have $|\lambda_{\pm}| < 1$ for $0 < \kappa < \pi/2$, which means the presence of the edge mode in the whole region of positive κ . With $\kappa < 0$, there appears a reentrant edge mode near the zone boundary $\kappa = -\pi/2$, which is not seen in the upper panel because of its much lower energy. The binding energy of reentrant edge mode near zone boundary is expanded as

$$E_{\uparrow} - E_b \sim -4\Delta_B \left(\frac{D+1}{A}\right)^2 \left(\kappa + \frac{\pi}{2}\right)^2. \quad (68)$$

The reentrant mode merges with bulk excitations at momentum κ_m that is given by the solution of

$$\begin{aligned} & (\Delta_B + 4 \cos \kappa) \cos \theta - \sqrt{2}A \sin \kappa \sin \theta \\ & = \Delta_B \cos \theta + 2R = 0. \end{aligned} \quad (69)$$

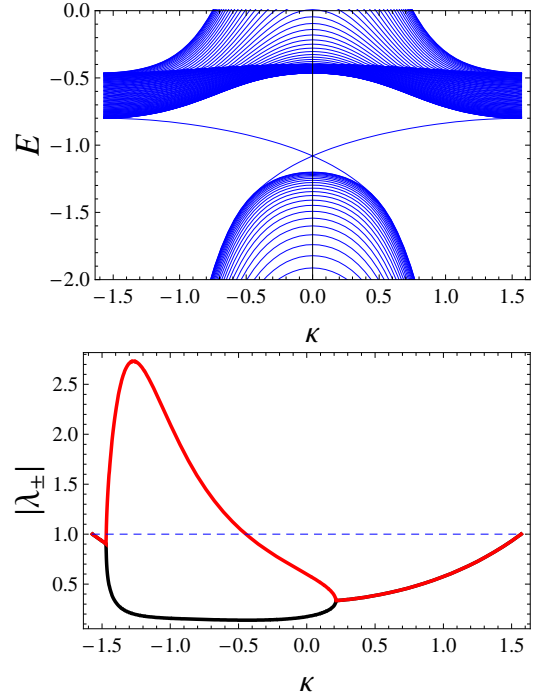


FIG. 8. (Color online) Energy spectrum $E(\kappa)$ and parameters $|\lambda_{\pm}|$ in zigzag edge system with $\Delta = 1.2$, $A = 1$, $D = 0.9$.

The analytic expression of κ_m in terms of system parameters is complicated and it's not illuminating. For the parameters used in Fig.8, we obtain the numerical value: $\kappa_m = -0.936\pi/2$. Since κ_m is close to $-\pi/2$, the binding energy is only of the order of 10^{-3} according to Eq.(68). The reentrant mode vanishes also at the zone boundary because of the relation: $|\lambda_{\pm}| \rightarrow 1$ as $\kappa \rightarrow -\pi/2$.

In critical case with $D = 1$, the bulk energy gap closes, with extremum of E_b given by

$$E_{b+}|_{min} = E_{b+}(\pi/2, \pi/2) = -\Delta \quad (70)$$

$$E_{b-}|_{max} = E_{b-}(0, 0) = -\Delta \quad (71)$$

Fig.9 shows the spectrum and parameters $|\lambda_{\pm}|$ in this case. Since we obtain $|\lambda_{\pm}(\kappa = 0)| = 1$ with $D = 1$, the crossing point of two helical edge modes merges with bulk excitations associated with indirect gap-closing. However, edge mode still exists in the other momentum region with $|\lambda_{\pm}| < 1$. Note that the right-going helical mode has the flat spectrum for $\kappa > 0$, and that the left-going helical mode has the flat spectrum for $\kappa < 0$,

With $D > 1$, the system is no longer a topological insulator. However the edge mode still survives in some momentum region. Fig.10 shows the spectrum and parameters $|\lambda_{\pm}|$ in this case. The edge mode contains two separate parts lying near the zone boundary in valence and conduction bands. This new phase is bulk metal but with helical edge mode. Note that the solution $\sin \theta$ becomes complex in certain momentum region, which is unphysical.

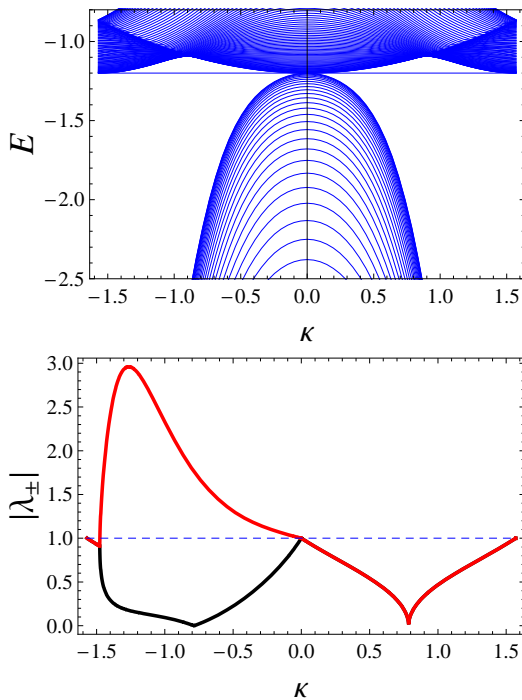


FIG. 9. (Color online) The same quantities as in Fig.8 except for $D = 1$ in this case.

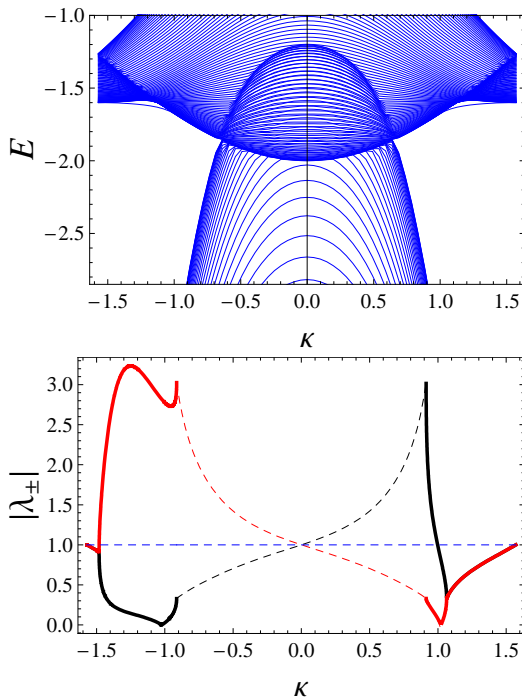


FIG. 10. (Color online) The same quantities as in Figs.8 and 9 except for $D = 1.1$ in this case. The dashed lines in the lower panel correspond to complex $\sin \theta$ which is unphysical.

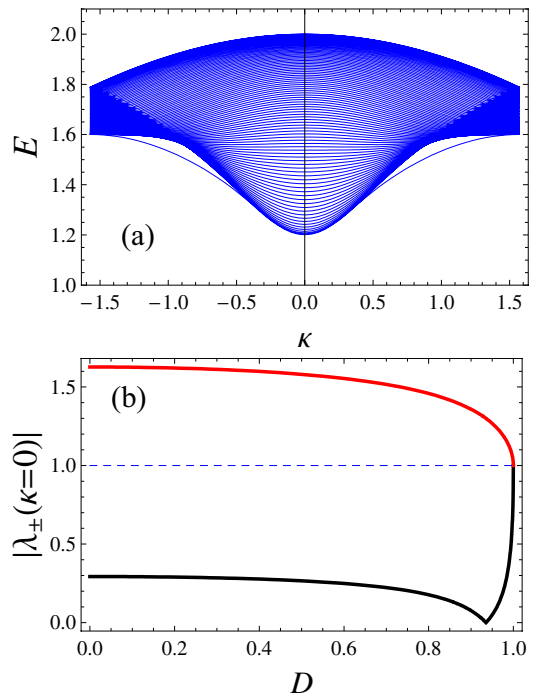


FIG. 11. (Color online) (a) Conduction band $E(\kappa)$ with $\Delta = -1.2$, $A = 1$, $D = 0.9$ in zigzag edge system. (b) Parameter $|\lambda_{\pm}(\kappa=0)|$ as a function of D .

Let us now consider the OI case with $\Delta = -1.2$. According to Eq.(67), edge mode will appear near the boundary of BZ. Fig.11 (a) shows an example of the spectrum (upper panel). There is no edge mode within the energy gap. Fig.11 (b) shows the absence of the edge mode at $\kappa = 0$, since at least one of the $|\lambda_{\pm}|$ is larger than unity.

V. SUMMARY

In this paper, we have analyzed edge modes in the particle-hole asymmetric BHZ model taking both straight and zigzag edges. Our particular attention has been the survival or disappearance of helical edge modes through transition from TI to SM, and also its presence in OI.

For straight edge, with increasing particle-hole asymmetry controlled by D , the edge mode breaks up into two parts in momentum space, and each part shrinks simultaneously. Associated with transition from TI to SM, the system becomes normal SM without edge mode. On the other hand, in zigzag edge case, helical edge mode is robust against particle-hole symmetry breaking. In TI, gapless point always lies at the Γ point and reentrant edge mode appears near the boundary of 1D BZ. With closing of indirect gap in bulk energy band, those edge modes near the crossing point of Kramers' pair disappear, while the edge mode near the zone boundary remains.

In OI systems, helical edge mode, if exists, should not be inside the energy gap. Then such edge mode does not change the topology of energy band from OI without edge modes. In straight edge system, the presence of edge mode is sensitive to parameters. However, for zigzag edge case, it is insensitive to values of parameter because the edge mode always merges with bulk modes at the zone

boundary.

In summary, we have demonstrated the presence of helical edge modes outside the energy gap as a novel state in particle-hole asymmetric BHZ model. Our analytic approach to study the helical modes can be generalized to 3D systems. The results will be reported elsewhere.

-
- [1] C. Wu, B.A. Bernevig, and S.C. Zhang: Phys. Rev. Lett. 96, 106401 (2006).
 - [2] C. Xu and J. Moore: Phys. Rev. B 73, 045322 (2006).
 - [3] D. Hsieh, Y. Xia, L. Wray, D. Qian, A. Pal, J.H. Dil, J. Osterwalder, F. Meier, G. Bihlmayer, C.L. Kane, Y.S. Hor, R.J. Cava, and M.Z. Hasan: Science 323, 919 (2009).
 - [4] D. Hsieh, L.A. Wray, D. Qian, Y. Xia, Y.S. Hor, R.J. Cava, and M.Z. Hasan: arXiv:1001.1574.
 - [5] A.A. Taskin and Y. Ando: Phys. Rev. B 80, 085303 (2009).
 - [6] A.A. Taskin, K. Segawa, and Y. Ando: Phys. Rev. B 82, 121302 (2010).
 - [7] Y.S. Hor, P. Roushan, et al.: Phys. Rev. B 81, 195203 (2010).
 - [8] J.G. Analytix, J.H. Chu, Y. Chen, F. Corredor, R.D. McDonald, Z.X. Shen, and I.R. Fisher: Phys. Rev. B 81, 205407 (2010).
 - [9] K. Eto, Z. Ren, A.A. Taskin, K. Segawa, and Y. Ando: Phys. Rev. B 81, 195309 (2010).
 - [10] H. Zhang, C.X. Liu, X.L. Qi, X. Dai, Z. Fang and S.C. Zhang: Nat. Phys. 5, 438 (2009).
 - [11] B. A. Bernevig, T. L. Hughes and S.C. Zhang: Science 314, 1757 (2006).
 - [12] B. Zhou, H.Z. Lu, R.L. Chu, S.Q. Shen, and Q. Niu: Phys. Rev. Lett. 101, 246807 (2008).
 - [13] E.B. Sonin: Phys. Rev. B 82, 113307 (2010).
 - [14] M. König, H. Buhmann, L.W. Molenkamp, T.L. Hughes, C.X Liu, X.L Qi and S.C Zhang: J. Phys. Soc. Jpn **77**, 031007 (2008).
 - [15] K. Imura, A. Yamakage, S.J. Mao, A. Hotta and Y. Kuramoto: Phys. Rev. B 82, 085118 (2010).
 - [16] S.J. Mao, Y. Kuramoto K. Imura, and A. Yamakage: arXiv:1008.0481; J. Phys. Soc. Jpn in press.
 - [17] S. Murakami: arXiv:1006.1188.
 - [18] M. Creutz and I. Horvath: Phys. Rev. D 50, 2297 (1994).
 - [19] M. Creutz: Rev. Mod. Phys. 73, 119 (2001).